AIP Conference Proceedings

RESEARCH ARTICLE | JULY 15 2025

Water shock when starting pumps in automated pumping stations

Sobir Jonkobilov ✉; Bektemir Jonkobilov; Shohruh Bahodirov; Jahongir Ruzikulov; Murodilla Ulugmuradov

AIP Conf. Proc. 3256, 020034 (2025)
https://doi.org/10.1063/5.0267000

Water shock when starting pumps in automated pumping stations

Sobir Jonkobilov[1, 2, a)], Bektemir Jonkobilov[2, b)], Shohruh Bahodirov[1, c)], Jahongir Ruzikulov[1, d)], and Murodilla Ulugmuradov[1, e)]

[1]*Karshi institute of irrigation and agrotechnologies, Karshi, 180119, Uzbekistan*
[2]*Karshi engineering economic institute, Karshi, 180100, Uzbekistan*

[a)] Corresponding author: jonkobilovsobir@gmail.com
[b)] bektemirzonkobilov@gmail.com
[c)] bahodirovshohrux2613@gmail.com
[d)] jahonruziqulov06@gmail.com
[e)] ulugmuradovmurod@gmail.com

Abstract. The article is devoted to the study of water hammer when starting pumps in automated pumping stations with low inertia of moving masses and taking into account pressure losses when filling the elastic capacity of the pipeline. The article provides an analysis of scientific works devoted to the determination of shock pressure during the startup of pumping stations. The article presents an analytical study of shock pressure during the startup of automated pumping stations, which provides an accurate assessment of the optimal parameters of pumping units and pressure systems. The article obtained dependence for calculating the shock pressure when starting up automated pumping stations, taking into account energy loss along the length of the pipeline; it increases the reliability of the pressure system and ensures resource saving when designing pressure-hydraulic systems. A graphic-analytical method is proposed to determine the shock pressure during a hydraulic shock when starting a pump with an open valve installed at the beginning of the pressure pipeline. The results of theoretical studies are compared with experimental data on shock pressures when starting the main pumps of pumping stations. At the same time, a reliable agreement was obtained between the results of calculations of pressure pipelines based on the proposed dependence on water hammer and experimental data.

Keywords: Shock pressure, inertia of the water mass, pump with low inertia, shock characteristics of the pipeline, pressure characteristics of the pump.

INTRODUCTION

Currently, the theory of water hammer in pressure pipelines has been developed and supplemented in the scientific works of H.A.Kaveh [1], D.Kraiem [2], M.Fersi [3], A.Triki [4], T.Chen [5], D.Covas [6], and many others.

Despite many years of studying water hammers, there are still issues in this area of fluid mechanics that require further research. In automated pumping stations, the pumps start with the valve on the open pressure pipeline. At the same time, hydraulic shocks often occur in pressure pipelines, which, as studies conducted at the Kungirtag pumping station in the Kashkadarya region, show, in most cases, even exceed the shocks when the units stop. Meanwhile, until recently, detailed studies of water hammers when pumping units were not sufficiently carried out since previously, the pumps were started with the valve closed and then slowly opened [7-9].

Currently, in automated pumping stations, to simplify and reduce the cost of automatic control equipment, pumps are usually started and stopped with the valve on the pressure line open. During the period of transition processes, i.e., when starting and stopping pumps, hydraulic shocks are often observed in pipelines, which, under certain conditions, can reach significant values. In the scientific literature, there are indications that more than 80% of all damage in pipelines is caused by the destructive effect of hydraulic shocks [10, 11]. According to our observations, water leaks on such pipelines are growing from year to year.

When starting a pump, as well as when operating a valve, two different cases of water hammer can be observed.

Water, Energy and Food Security in the Context of Global Climate Change and Water Scarcity
AIP Conf. Proc. 3256, 020034-1–020034-9; https://doi.org/10.1063/5.0267000
Published under an exclusive license by AIP Publishing. 978-0-7354-5198-8/$30.00

If the pump has low power, then it usually has low inertia of the moving masses and, therefore, accelerates to normal speed and normal pressure in a very short time. If, in addition, the length of the pipeline is sufficiently large, then the pump acceleration time is less than the full impact phase $t = 2l/a$; therefore, the hydraulic shock at start-up is similar to the case of a direct impact [12, 13].

MATERIALS AND METHODS

Special studies were carried out to experimentally test the hydraulic shock in the pressure pipeline of the Kungirtag pumping station in the Kashkadarya region when starting the pump in order to test the proposed calculation methodology, the methodology for which is set out in works. The pumping station is shown in Fig. 1.

FIGURE 1. Pumping station "Kungirtag" Kashkadarya region.

The experimental study was carried out by measuring the shock pressure when starting the pump at the Kungirtag pumping station in the Kashkadarya region. The diameter and length of the pressure pipeline is D_y=200 mm and z = 2200 m. The source of the pumping station is the Pistali channel. Pump brand D500-65. The pump flow was determined according to the pump's operating characteristics, which are given in the pump passport. The following instruments and equipment were used to record static and shock pressures [8, 9].

Primary membrane pressure transducer (sensor). Manufacturer: DFROBOT (China). A specially developed intelligent pressure sensor (secondary converter) (Calibration protocol. Protocol number UZ-14/----2021. National Metrological Institute of Uzbekistan. Laboratory "Measurement of flow and pressure of liquid and gas."). A signal about a change in hydrodynamic pressure during an impact from an intelligent converter (IDD-1) is sent directly to a laptop computer [8, 9].

The initial pressure before the impact was determined using standard pressure gauges of accuracy class 1. An intelligent pressure sensor (secondary transducer) was used to record pressures during water hammer [8, 9].

The operation of the pressure sensor is based on changes in the inductance of the system when pressure changes. The sensor membrane, which senses pressure, is the anchor of the inductive system; moreover, the pressure sensor has two windings, working and compensating, which are included in IPD-1 (intelligent pressure sensor). The pressure sensor allows multiple pressure overloads [8, 9].

IDD-1, which includes an amplifier-converter, is a two-channel device and, complete with a pressure sensor, is intended for measuring rapidly changing pressures in various pneumatic and hydraulic systems.

The resulting diagrams of hydrodynamic pressures during impact were recalculated using calibration graphs. Calibration of pressure sensors at the experimental stand of Uzstandart RUz was carried out using the static method "for injection" and "for discharge" [8, 9].

The measurement error of the pressure sensor is 0.5-1.0%. The signal from the pressure sensor, amplified and converted by IDD-1, was sent to the computer. The parameters of the steady-state and unsteady modes during the experiment were recorded on a computer. Pressure during steady motion was measured with standard MO-1227 pressure gauges with an accuracy class of 0.15 to 1.5 MPa [8, 9].

The accuracy of pressure measurement was

$$\Delta P = 0.015 \cdot 1.5 = 0.00225\ MPa = 2.25\ kPa$$

The initial pressure in the pressure pipeline varied in the range of 0.1 – 0.6 MPa; this range corresponds to a relative measurement error of 0.375-2.25%.

RESULTS AND DISCUSSION

As a result of the research, a diagram of the hydraulic shock when starting the pump was obtained and recorded by the pressure indicator IDD-1 [8, 9] at the Kungirtag pumping station in the Kashkadarya region (Fig. 2).

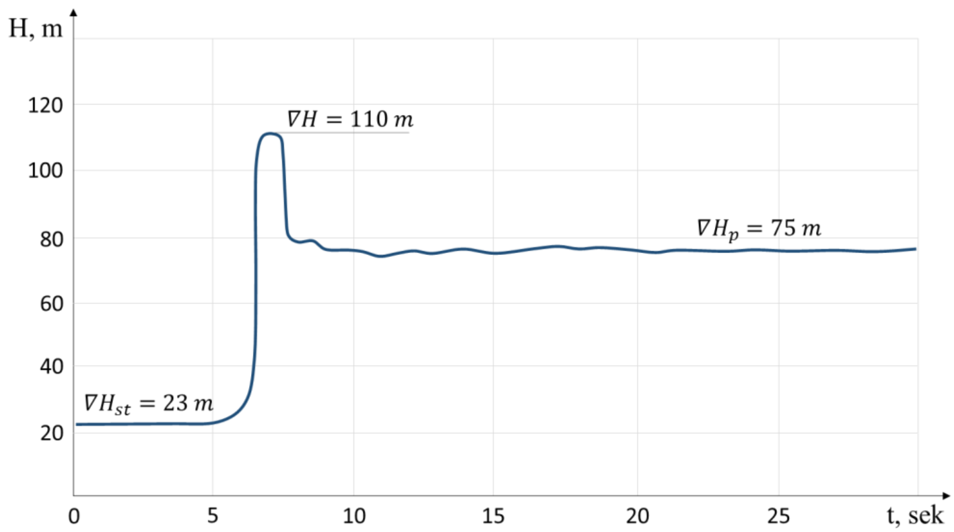

FIGURE 2. Diagram of water hammer when starting a pump at the Kungirtag pumping station in Kashkadarya region.

Sufficiently powerful pumping units have a large inertia of moving parts and, therefore, gain speed relatively slowly; if, in addition, the length of the pressure pipeline is small, then the pump may not have time to develop full pressure before the waves of pressure reduction reflected from the reservoir approach it at a later time $t = 2l/a$. In this case, similar to an indirect shock, the water hammer at start-up will be mitigated. The water supply system mainly uses low-power pumps (up to 50-100 kW) with low inertia of moving masses, and the length of pressure lines often reaches 2-4 km, so hydraulic shocks during startup are noticeable here [10-12]. The phenomenon of the water hammer when starting such a pump occurs as follows. After overcoming the static pressure, the check valve opens, and water from the pump begins to flow into the pipeline. However, a normal steady flow does not immediately occur here because the water, due to its inertia, acts like a covered valve. Therefore, the pressure in the pipeline rises above the operating pressure but not above the maximum pressure that the pump can develop according to its characteristics. This rise in H during pump startup is called a water hammer. Under pressure H, the so-called free or elastic capacity of the pipeline is initially filled with water, i.e., the space formed due to compression of water when pressure rises and expansion of the open cross-section of pipes. The increased pressure and, as a consequence, compression of the liquid and deformation of the pipe walls with shock wave speed propagate along the entire pipeline [14-16]. Having been reflected from the reservoir, the increased pressure is destroyed, and then, at the same speed, the operating pressure and normal speed are established towards the pump [17-21].

Water hammers were studied when starting a pump [9]. The author has proven through experiments that the hydraulic shock at start-up does not exceed the maximum pressure that the pump develops with a small water supply according to its characteristics [9]. The exact magnitude of the hydraulic shock when starting the pump has not been determined [9].

In [11], a theoretical explanation is given for the process of hydraulic shock during startup with sick inertia of moving masses. For these pumps, the author [11] proposed an approximate calculation method. However, noticeable hydraulic shocks are not observed when starting powerful pumps.

The author [11] for pumps with low inertia proposed a method for calculating hydraulic shock at start-up based on the use of empirical coefficients. Still, their actual values have not yet been established.

The author proposed a graphical-analytical method for determining shock pressure when starting a pump with low inertia of moving masses and taking into account pressure losses when filling the elastic container of the pipeline.

The initial equation is taken to be the pump characteristic q-H_m, where H_m is the gauge pressure of the pump, and the basic equation of the water hammer takes into account energy losses. When plotting these equations graphically, the point where they intersect shows the likely shock pressure when starting the pump.

Some difficulties are caused by the fact that the pump catalogs provide characteristics where H is the total pressure of the pump, taking into account the vacuum suction height. For the calculation, you can use an approximate construction of the pump characteristic q-Hm by reducing all ordinates of the q-H curve by the value of the permissible vacuum suction height H_{vac}^{per}, also given in the catalogs, or conditionally assume that $H_M \approx H$, since $H_M >> H_{vac}$. Both methods are approximate, but their use does not result in significant errors.

To derive the shock characteristics of the pipeline taking into account losses, consider the diagram shown in Fig. 3. When the pump is started, due to the inertia of the mass of water in the pipeline, shock pressure H arises near the pump, which is spent on overcoming the static pressure H_{st}, inertial pressure h_i and pressure losses $h_c^{'}$ when filling the elastic capacity of the pipeline with a variable speed ϑ, that is, it is known from the hydraulics course that

$$H = H_{st} + h_i + h_l \quad (1)$$

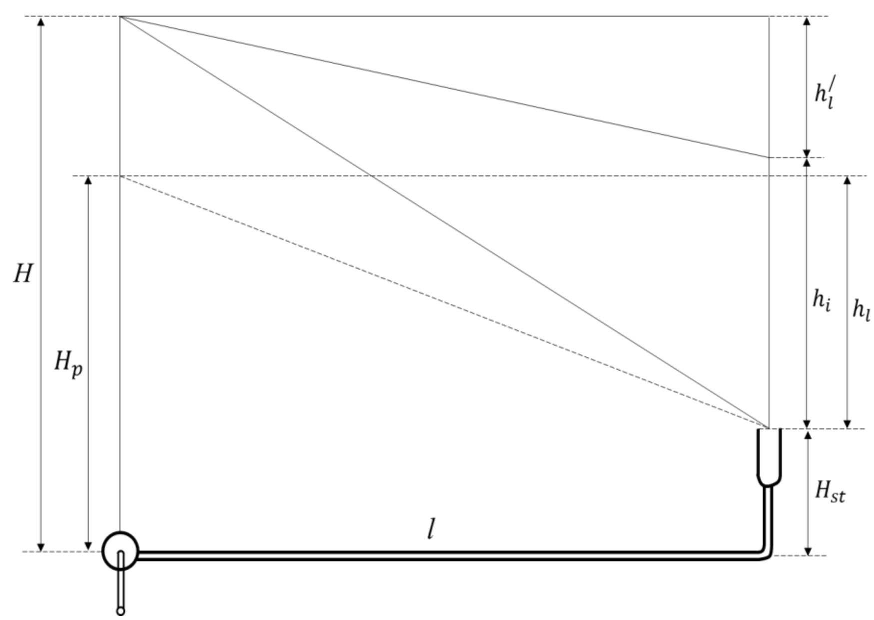

FIGURE 3. Diagram explaining water hammer when starting pump.

$$h_i \approx \frac{l d\vartheta}{g\, dt} \quad (2)$$

$$h_l^{/} = \lambda \frac{l\vartheta^2}{d 2g} = \zeta \frac{\vartheta^2}{2g} \quad (3)$$

where ζ is the system resistance coefficient.

Then

$$H = H_{st} + \frac{l d\vartheta}{g dt} + \zeta \frac{\vartheta^2}{2g} \quad (4)$$

where

$$dt = \frac{l d\vartheta}{g\left(H - H_{st} - \zeta \frac{\vartheta^2}{2g}\right)} \tag{5}$$

Equation (5) includes three variables, so we will additionally use the flow continuity equation when filling the elastic capacity of the pipeline:

$$dW = \vartheta \omega dt \tag{6}$$

where dW is the elementary volume of liquid supplied to the pumps into the pipeline during time dt; ω is the open cross-sectional area of the pipe.
It can be proven that

$$dW = \frac{l\omega g}{a^2} dH \tag{7}$$

a similar formula was obtained in [11].

Equating the right-hand sides of equations (6) and (7), we obtain

$$\frac{\lg}{a^2} dH = \vartheta dt \tag{8}$$

Expression (5) is substituted into the last equation, then

$$\frac{g^2 dH}{a^2} = \frac{\vartheta d\vartheta}{H - H_{st} - \zeta \frac{\vartheta^2}{2g}} \tag{9}$$

The differential equation (9) is the basic equation of water hammer taking into account energy losses when filling the elastic capacity of pressure systems. To prove this, let us assume that energy losses are zero, that is, ζ=0 then

$$\frac{g^2 dH}{a^2} = \frac{\vartheta d\vartheta}{H - H_{st}} \tag{10}$$

where

$$\vartheta d\vartheta = \frac{g^2}{a^2}(H - H_{st}) dH$$

let's integrate the last equation:

$$\int_0^{\vartheta_0} \vartheta d\vartheta = \frac{g^2}{a^2} \int_{H_{st}}^{H} (H - H_{st}) dH \, ,$$

$$\frac{\vartheta_0^2}{2}=\frac{g^2}{a^2}\left|\frac{H^2}{2}-H_{st}H\right|_{H_{st}}^{H}$$

or

$$\frac{\vartheta_0^2}{2}=\frac{g^2}{a^2}\left(\frac{H^2-H_{st}^2}{2}-H_{st}H+H_{st}^2\right)$$

where

$$\frac{a^2\vartheta_0^2}{g^2}=H^2-H_{st}^2-2H_{st}H+2H_{st}^2=\left(H-H_{st}\right)^2.$$

Hence

$$H=H_{st}+\frac{\alpha\vartheta_0}{g} \tag{11}$$

As a result, we obtained a formula for calculating the maximum pressure during a water hammer, which does not take into account energy losses in the pressure pipeline.

The differential equation (9) with no separable variables is generally nonlinear since $\zeta=f(\vartheta)$; therefore, its integration presents significant difficulties. If we assume that the filling of the elastic capacity of the pipeline occurs in a turbulent mode in the quadratic resistance region, as is usually the case in reality, then the λ and ζ coefficients do not depend on the speed ϑ, and then equation (9) can be reduced to the form of a differential equation D. Bernoulli:

$$\frac{d\vartheta}{dH}+\zeta\frac{\vartheta g}{2a^2}=\frac{g^2\left(H-H_{st}\right)}{a^2}\vartheta^{-1} \tag{12}$$

The last equation can be easily integrated using methods known in mathematics. As a result of integration, the following equation is obtained:

$$\vartheta=\sqrt{\frac{2g}{\zeta}\left(H-\frac{a^2}{g\zeta}-H_{st}\right)+\frac{2a^2}{\zeta^2\exp\left[\zeta\frac{d}{a^2}\left(H-H_{st}\right)\right]}} \tag{13}$$

The application of the proposed methodology is explained in detail in the following example.

Example. A working pump D500-65 is installed at the Kungirtag pumping station; N=92 kW; n=1000 rpm. This pump supplies water with a flow rate of q=430 m^3/h to the pressure pool through a pressure pipeline with a length of l=2200 m. The pressure line has a diameter of d=200 mm. The live cross-sectional area of the pressure line is ω_{ob}=0.134 m^2. Shock wave propagation speed, a=1030 m/sec. This speed is achieved by good removal of air from the pressure pipeline through the occurrence of hydraulic shocks at low water velocities in the pressure system. Static pressure H_{st}=45 m, working pressure H_p=85 m. The pump characteristics are shown in Fig. 3. The vacuum suction lift was not taken into account here.

When calculating, we assume that the filling of the elastic capacity of pressure systems occurs in a turbulent mode in the quadratic resistance region, then according to the Darcy formula

$$h_0=\zeta\frac{\vartheta_0^2}{2g}$$

we get

$$\zeta=\frac{2gh_0}{\vartheta_0^2}$$

where h_0 is the pressure loss during steady flow: $h_0 = H_p - H_{st} = 85 - 45 = 40\ m$.

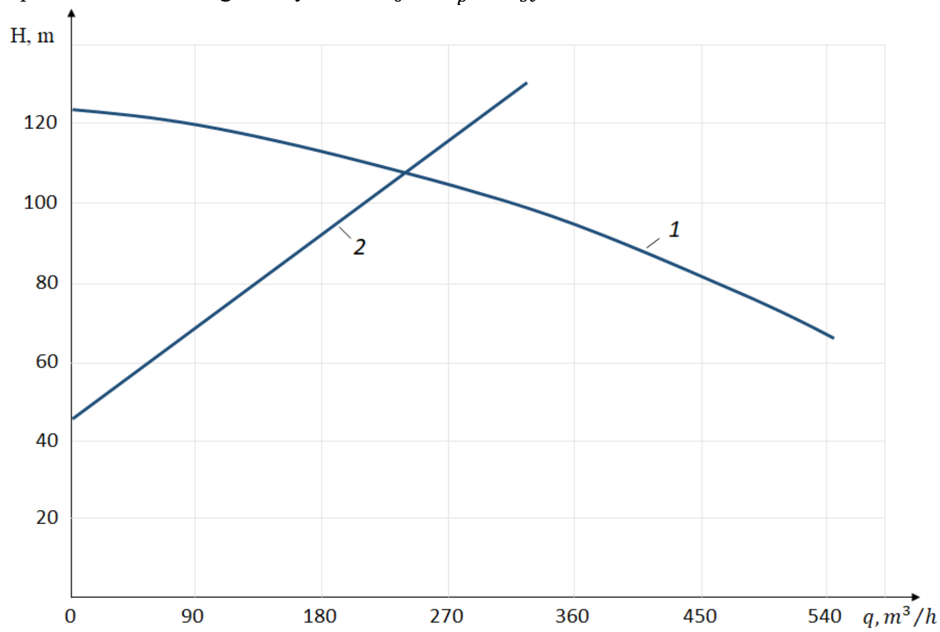

FIGURE 4. Determination of shock pressure when starting pump using graphic-analytical method: 1 is characteristics of the D500-36 pump; 2 is shock characteristic of the pipeline according to formula (13).

$$\vartheta_0 = \frac{q}{3600\omega_{total}} = \frac{430}{3600 \cdot 0.134} \approx 0.89 \text{ m/sec}$$

Then

$$\zeta = \frac{2 \cdot 9.81 \cdot 40}{0.892} \approx 1000.$$

The known values of ζ, a, H_{st}, and d are substituted into equation (13), which then takes the form

$$\vartheta = \sqrt{0.0197(H - 153.3) + 2.12e^{-0.00924(H-45)}} \quad (14)$$

Having specified several values of H, the speed ϑ and then the flow rate $q = 3600\omega_{total}\vartheta$ are calculated using formula (14).

Calculations are given in Table 1. According to Table 1, curve 2 is plotted on the graph with the characteristics of pump 1 (Fig. 4). It should be borne in mind that at $\vartheta = 0$, $H = H_{st} = 45$ m. The intersection point of these curves shows the impact pressure H=109 m. According to actual measurements, it was equal to H≈115 m. The small discrepancy is apparently explained by the fact that the pump during the startup process developed a speed greater than the calculated one.

Using formula (11) to calculate water hammer without taking into account pressure losses instead of formula (12) in this case gives an insignificant difference. However, this is not always the case. At speeds $\vartheta_0 > 1.0$ m/sec, the discrepancy between the results according to formulas (11) and (12) can be significant.

TABLE 1. Calculation of water hammer parameters when starting pump using formula (14)

H, m	**0.0197(H-1533)**	**0.00924(H-45)**	**$2.12e^{-0.00924(H-45)}$**	***ϑ, m/sec***	***$q, m^3/h$***
180	-1.45	-0.322	1.53	0.280	134
100	-1.06	-0.509	1.26	0.445	212
130	-0.484	-0.786	0.96	0.675	324

The hydraulic shock when starting pumps does not exceed the maximum pressure developed by the pump. Therefore, a misconception may be created that such impacts are not dangerous for the pipeline. However, a study of the characteristics of pumps produced by industry shows that many pumps with steep characteristics are capable of developing pressures significantly higher than operating pressures during startup. This circumstance should be taken into account when making calculations. In addition, frequent and rather strong pressure fluctuations in pressure pipelines at automated pumping stations disrupt the tightness of joints, which causes water leaks.

CONCLUSIONS

Based on the above, the following conclusions can be drawn:

As a result of the theoretical solution of differential equations of unsteady motion of a real fluid, a dependence was obtained for calculating the shock characteristics of a pressure pipeline, taking into account pressure losses.

A graphical-analytical method is proposed for calculating the shock pressure when starting a pump in a pressure pipeline during a hydraulic shock.

The results of theoretical calculations based on the proposed dependence are compared with experimental data on shock pressures when starting the main pumps of pumping stations. At the same time, a reliable coincidence of the results of calculations of pressure pipelines according to the proposed dependence on water hammer with experimental data was obtained.

REFERENCE

1. Kaveh, H. A., Faig, B. O. N. & Akbar, K. H. 2010 Some aspects of physical and numerical modeling of waterhammer in pipelines. Nonlinear Dynamics 60, 677–701. https://doi.org/10.1007/s11071-009-9624-7.
2. Dalila Kraiem & Ali Triki. (2023) Tackling of hydraulic cavitation in pressurized pipe flow using high- or low-density polyethylene penstock and short-section. *AQUA — Water Infrastructure, Ecosystems and Society* 72:11, pages 2126-2137. https://doi.org/10.1080/09715010.2023.2227593.
3. Fersi, M. & Triki, A. 2023 Removal of cavitation using HDPE/LDPE inline section-pipe. Journal of Pressure Vessel Technology Transactions of the ASME 145 (2), 024501. https://doi.org/10.1115/1.4055155.
4. Fersi, M. & Triki, A. 2019a Investigation on re-designing strategies for water-hammer control in pressurized-piping systems. Journal of Pressure Vessel Technology Transactions of the ASME 141(2), 021301. https://doi.org/10.1115/1.4040136.
5. Chen, T., Ren, Z., Xu, C. & Loxton, R. 2015 Optimal boundary control for water hammer suppression in fluid transmission pipelines. Computers & Mathematics with Applications 69 (4), 275–290. https://doi.org/10.1016/j.camwa.2014.11.008.
6. Covas, D., Stoianov, I., Ramos, H., Graham, N., Maksimovic, C. & Butler, D. 2004 Water-hammer in pressurized polyethylene pipes: Conceptual model and experimental analysis. Urban Water Journal 1 (2), 177–197. https://doi.org/10.1080/15730620412331289977.
7. Alberto J., Conejero, Lizama C., Rodenas F. Dynamics of the solutions of the water hammer equations [J]. Journal of Topology and its Applications, 2016, (203): 67–83. https://doi.org/10.1016/j.topol.2015.12.076.
8. A. Arifjanov, U Jonqobilov, S Jonqobilov, SH Khushiev, J Xusanova. The influence of hydraulic friction on the maximum pressure of water hammer. ICECAE 2020, IOP Conf. Series: Earth and Environmental Science 614 (2020) 012092, IOP Publishing, doi:10.1088/1755-1315/614/1/012092.
9. Arifjanov A.M., Jonkobilov U.U., Jonkobilov S.U., Bekjonov R.S. The Hydraulic Impact Wave Propagation Speyed Study in a Two-Phase Flow. International Journal for Innovative Engineering and Management Research. (9)11 (2020) 94-100. https://doi.org/10.48047/IJIEMR/V09/I11/19.
10. Bergant, A., Simpson, A. R. & Tijsseling, A. 2006 Water-hammer with column separation: A historical review. Journal of Fluids and Structures 22 (2), 135–171. https://doi.org/10.1016/j.jfluidstructs.2005.08.008.
11. Besharat, M., Tarinejad, R. & Ramos, H. M. 2016b The effect of water hammer on a confined air pocket towards flow energy storage system. Journal of Water Supply: Research and Technology – AQUA 65, 116–126. https://doi.org/10.2166/aqua.2015.081.
12. Asli K.H., Naghiyev A.K. Some aspects of physical and numerical modeling of water hammer in pipelines, Nonlinear Dynam. 60 (4) (2010) 677-701. https://doi.org/10.1007/s11071-009-9624-7.
13. Bergant, A., Tijsseling, A.S., Vitovsky, J.P., Covas, D.I.C., Simpson., A.R., Lambert, M.F., Parameters affecting water hammer wave attenuation, shape and timing. Part 1: Mathematical tools. J. Hydraul. Res. 46(3)

(2008) 373-381.
14. Bertaglia G., Ioriatti, A. Valiani M., Dumbser M., Caleffi V., Numerical methods for hydraulic transients in visco-elastic pipes, J. Fluid Struct. 81(C) (2018) 230-254. https://doi.org/10.1016/j.jfluidstructs.2018.05.004.
15. Besharat M., Tarinejad R., Aalami M.T., Ramos H. Study of a compressed air vessel for controlling the pressure surge in water networks: CFD and experimental analysis, Water Resour. Manag. 30 (8) (2016) 2687-2702. https://doi.org/10.1007/s11269-016-1310-1.
16. Bojan Ivljanin, Vladimir D. Stevanovic, Aleksandar Gajic. Water hammer with non-equilibrium gas release. International Journal of Pressure Vessels and Piping, 165 (2018) 229-240. https://doi.org/10.3390/w15101942.
17. Daude F., Tijsseling A.S., Galon P., Numerical investigations of water-hammer with column-separation induced by vaporous cavitation using a one-dimensional Finite Volume approach, J. Fluid Struct. 83 (2018) 91-118. https://doi.org/10.1016/j.jfluidstructs.2018.08.014.
18. Ghidaoui M.S., Zhao M., Duncan A.M., David H.A. A review of water-hammer theory and practice, Appl. Mech. Rev. 58 (2005) 49-76. https://doi.org/10.1115/1.1828050.
19. Guo L. L., Geng J., Shi S. et al. Computing research of the water hammer pressure in the process of the variable speed closure of valve based on UDF method, J. Journal of Shandong University (Natural Edition), 49(3) (2014) 27-30. https://doi.org/10.1145/3305275.3305303.
20. Henclik S. Numerical modeling of water hammer with fluid-structure interaction in a pipeline with viscoelastic supports, J. Fluids Struct. 76 (2018) 469-487. https://doi.org/10.1016/j.jfluidstructs.2017.10.005.
21. Triki A., Further investigation on water-hammer control inline strategy in watersupply systems, J. Water Supply Res. Technol. Aqua 67(1) (2018) 30-43. https://doi.org/10.2166/aqua.2017.073.